IOP Publishing | Bureau International des Poids et Mesures Metrologia

Metrologia **54** (2017) 280–289 https://doi.org/10.1088/1681-7575/aa62e3

Final determination of the Boltzmann constant by dielectric-constant gas thermometry

Christof Gaiser[1], Bernd Fellmuth, Norbert Haft, Axel Kuhn, Bettina Thiele-Krivoi, Thorsten Zandt, Joachim Fischer, Otto Jusko and Wladimir Sabuga

Physikalisch-Technische Bundesanstalt (PTB), Abbestrasse 2-12, 10587, Berlin and Bundesallee 100, 38116 Braunschweig, Germany

E-mail: christof.gaiser@ptb.de

Received 17 January 2017, revised 21 February 2017
Accepted for publication 24 February 2017
Published 30 March 2017

Abstract

Gaiser *et al* published in 2013 (*Metrologia* **50** L7–11) a second, improved value of the Boltzmann constant k determined by dielectric-constant gas thermometry at the triple point of water ($k = 1.380\,6509 \times 10^{-23}$ J K^{-1}, relative standard uncertainty 4.3 parts per million (4.3 ppm)). Subsequently, the uncertainty was able to be reduced to 4.0 ppm by reanalysing the pressure measurement. Since 2013, further progress regarding this primary-thermometry method has been achieved in terms of the design and the assembly of the measuring capacitors, the determination of their effective compressibility, the sensitivity of the capacitance bridge, and the scattering and the evaluation of the data. Based on a huge amount of data, two new k values have been obtained by applying two different capacitors. The combination of these two values with the 2013 result, fully taking into account the correlations, has yielded a final result of $k = 1.380\,6482 \times 10^{-23}$ J K^{-1} with a relative standard uncertainty of 1.9 ppm. This value is about 0.2 ppm smaller than the CODATA 2014 one, which has a relative standard uncertainty of 0.57 ppm.

Keywords: Boltzmann constant, kelvin, units, thermometry, polarizability

(Some figures may appear in colour only in the online journal)

1. Introduction

The previous measurement of the Boltzmann constant k at the triple point of water (TPW) by dielectric-constant gas thermometry (DCGT) is described in detail in [1]. The result was $k = 1.380\,6509 \times 10^{-23}$ J K^{-1} with a relative standard uncertainty of 4.3 ppm. Subsequently, the uncertainty was able to be reduced to 4.0 ppm by reanalysing the pressure measurement [2, 3]. The fundamentals of DCGT as a primary-thermometry method, the details of the experimental setup, and the procedures for the evaluation of the data are described in detail in [3]. In the present paper, this information is not repeated fully. Rather, emphasis is given to the progress since 2013 in reducing the uncertainty by more than a factor of two, and to the data being the basis for deducing a final value of the Boltzmann constant.

To understand this paper it is only necessary to know the following facts about DCGT. The determination of k is based on measuring the pressure dependence of the capacitance of a capacitor containing the measuring gas, helium, at constant temperature, i.e. on measuring isotherms. The data pairs of pressure and relative capacitance change are fitted by applying a virial expansion that includes thermodynamic temperature as one of the parameters. In particular, the fitting coefficient of the first, linear term is given by $A_1 = (A_\varepsilon/RT + \kappa_{\mathrm{eff}}/3)^{-1}$, where A_ε is the molar polarizability, R is the molar gas constant, and T is the thermodynamic temperature. κ_{eff} denotes the effective compressibility of the capacitor, which describes the change of the capacitance due only to the mechanical deformation caused by

[1] Author to whom any correspondence should be addressed.

the measuring gas. T is traceable to the temperature of the TPW and κ_{eff} is calculated from the material parameters of the capacitor. Then, the ratio A_ε/R of two molar quantities is deduced from A_1 to determine k by applying the relation $k = (\alpha_0 \,/\, \varepsilon_0) \,/\, (3\, A_\varepsilon \,/\, R)$. The atomic dipole polarizability $\alpha_0 = 2.281\,513\ 31(23) \times 10^{-41}$ C m^2 V^{-1} in SI units is calculated *ab initio* with a relative standard uncertainty of 0.1 ppm [4]. The fixed electrical constant ε_0 and the Bohr radius published in [5] have been used.

The paper is organised as follows. In section 2, we describe the experimental setup, consisting of a large-volume thermostat, a vacuum-isolated measuring system, two tungsten carbide 10 pF cylindrical capacitors, an autotransformer ratio capacitance bridge, a high-purity gas-handling system including a mass spectrometer, and traceably calibrated special pressure balances with piston–cylinder assemblies having effective areas of 2 cm^2. The experimental results and the data evaluation including the uncertainty budget are discussed in detail in section 3. Section 4 deals with the determination of the final value of the Boltzmann constant k from the three values obtained for different capacitors considering all correlations. Finally conclusions are drawn. The mathematics used for deducing a weighted mean of k values considering the correlations is summarised in an appendix.

2. Experimental setup with improvements

2.1. Thermal conditions within a special thermostat

The measurement of the Boltzmann constant by DCGT requires one to determine the temperature of the gas and thus of the capacitor electrodes traceably to the definition of the base unit kelvin, i.e. to the temperature of the TPW, with a standard uncertainty of order 0.1 mK. To obtain a thermal environment of sufficient quality, a three-level arrangement has been realised in the DCGT experimental setup. Each capacitor is surrounded by a rigid, metallic pressure vessel, which is thermally anchored to the 30 mm thick central copper plate of the measuring system. For checking purposes, the temperature of the plate is measured with the aid of three capsule-type standard platinum resistance thermometers, which have been calibrated at the triple points of mercury and water as well as at the melting point of gallium. Besides the central plate at the bottom as a heat sink, the system consists of a top plate, four thick rods connecting the two plates and an isothermal shield, all made from copper, thus surrounding the capacitors. In turn, the measuring system is placed within a vacuum chamber for thermal isolation. Finally, the chamber is inserted in a huge liquid-bath thermostat. The thermal conditions within the experimental setup have been investigated in detail as described in three previous papers [6–8]. A photograph and a detailed design drawing of the measuring system are given in [6].

The liquid-bath thermostat has an overall volume of liquid of about 800 l and a central working volume, in which the vacuum chamber is located, with a diameter of 500 mm and a height of 650 mm. The temperature stability and the temperature field at the boundary of the working volume with and without the chamber have been investigated carefully under different experimental conditions. It can be verified that, under optimum conditions, both the instability and the inhomogeneity of the temperature in the working volume are well below 1 mK as necessary [7, 8].

Dedicated experiments described in [6, 7] have shown that the temperature of the central copper plate can be controlled well within 0.1 mK under steady-state conditions over time periods of a few days. Furthermore, the uncertainty component due to static temperature-measurement errors can be reduced to the same level. Special problems are caused by two unavoidable features of the DCGT experimental setup. First, during the experiments, the temperature of the capacitor electrodes inside the pressure vessels cannot be measured directly. It is not possible to place thermometers inside the vessels because of the requirement to guarantee a high purity of the helium gas. Second, due to the huge dimensions of the capacitors and the surrounding pressure vessels, the mass of the measuring system and thus its heat capacity are very large. This makes the thermal recovery of the system very slow, which is important for the measurements of isotherms. During such measurements, the flow of the measuring gas for changing the pressure inside the pressure vessel causes warming or cooling and thus temporary temperature changes. Both features require one to investigate the thermal recovery of the system in order to reduce dynamic temperature-measurement errors. Dedicated experiments have been performed by simulating the gas-flow-induced temperature changes via the application of heat pulses as discussed in [6, 7]. The experimental results are supported by theoretical calculations based both on simple rough models and finite-element methods (FEM). The obtained time constants of the thermal recovery have an order of magnitude of 1 h. The measurement of an isotherm lasts, therefore, at least several days. These recovery periods allow for deducing the temperature of the capacitor electrodes inside the pressure vessels with a standard uncertainty of order 0.1 mK. Under real experimental conditions, this theoretical description of the recovery is of course accompanied by a careful observation of the drift of the capacitance values with time.

2.2. Design of the measuring capacitors

A challenge for the determination of the Boltzmann constant k with DCGT is the deformation of the capacitor electrodes under the gas pressure, causing a disturbing additional capacitance change. To give an example: for a cylindrical capacitor as used here, ε_r of helium leads to a capacitance change of around 6.6×10^{-9} pF Pa^{-1}. The change caused by the decrease of the lengths of tungsten carbide electrodes is around -1×10^{-11} pF Pa^{-1} (in a cylindrical capacitor, the radial deformation cancels out). Thus, for a determination of k with a relative standard uncertainty of around 2 ppm, κ_{eff} has to be determined with the necessary small relative standard uncertainty of less than a tenth of a percent.

The cylindrical capacitors are sketched in figure 1. The two cylinders, which represent the inner and outer electrodes, are 100 mm long. The inner electrode has a diameter of 12 mm;

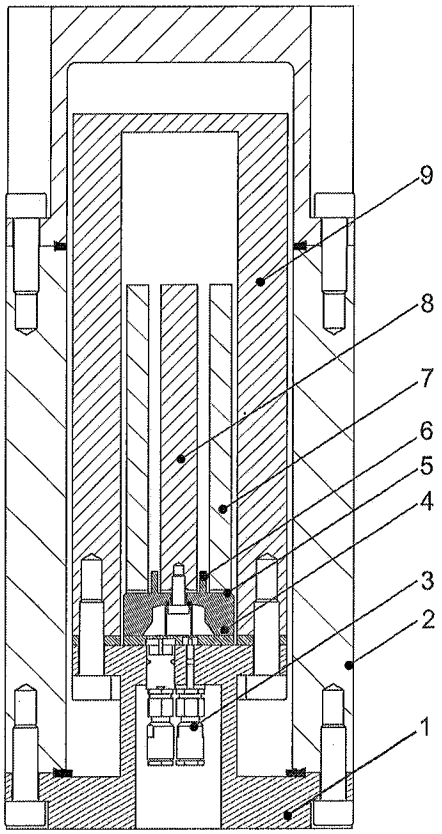

Figure 1. Final design of the 10 pF cylindrical composite capacitor assemblies TC2 and TC3: (1) vacuum flange (stainless steel); (2) pressure vessel connected to ground (stainless steel); (3) electrical feed-through; (4) bed-plate (tungsten carbide); (5) insulating discs (sapphire); (6) cylindrical ground-shield spacer; (7) outer electrode (tungsten carbide); (8) inner electrode (tungsten carbide); (9) massive shield (tungsten carbide).

the inner diameter of the outer electrode is 20 mm. To reduce edge effects, a small cylindrical ground-shield spacer (part of the bed-plate) exists at the bottom of the capacitor. The effective length $l = 93$ mm of the capacitors is given by the distance between the spacer at the bottom and the upper end of the electrodes. The electrodes are fixed on a grounded bed-plate. Electrical isolation is realized by sapphire (Al_2O_3) insulating discs (thickness 0.25 mm). Each electrode is connected with the capacitance bridge via coaxial cables and a feed-through, welded in the support plate of the surrounding vacuum-tight pressure vessel. The vessel for pressures up to 7 MPa has an inner diameter of 74 mm and an inner height of 233 mm.

The cylindrical electrodes, the ground-shield spacer (inner diameter 14 mm, length 7 mm) and the bed-plate, on which the electrodes are mounted, were made from tungsten carbide. This material has a compressibility that is by about a factor of two smaller than that of stainless steel used previously [9]. This led to a reduction of the uncertainty component caused by κ_{eff}. Furthermore, the relative displacement of the electrodes under pressure is reduced since the bed-plate is more rigid and its connection to the vacuum flange, which is bent by the gas pressure, is softer because the contact pressure of the screws is smaller than before. The mounting of the electrodes is improved by applying assembly tools. Since an eccentricity of the electrodes and an eccentric tilt both cause a change in κ_{eff} [10], their magnitudes were checked with a standard uncertainty of 1 μm using a coordinate measuring machine. Finally, on the basis of simulations with FEM, the ground shielding of the capacitor was optimised. The massive shield (see figure 1) was introduced in order to minimise the changes of stray capacitances due to the deformation of the electrodes, the shield and the pressure vessel by the gas pressure. This massive shield, already present in a prototype design around capacitor TC1 applied in [1], is the main change in the design compared to [9]. (Besides the individual mounting, TC1 is different from TC2 and TC3 only by the use of aluminium oxide isolating discs.) For the capacitors of the final design, no hysteresis could be detected during pressure cycling.

For the two new capacitors TC2 and TC3, electrodes from two different suppliers were used: TC2: Durit Hartmetall GmbH[2], TC3: Negele Hartmetall–Technik GmbH. (The electrodes of capacitor TC1 applied in [1] were from the same batch as those of capacitor TC2.) Both types of tungsten carbide are made of ultra-fine powder, leading to grain sizes less than 1 μm.

2.3. Determination of the effective compressibility

The effective compressibility describes the change of the capacitance due to the deformation and the relative displacement of the capacitor electrodes under pressure p. (In principle it is also influenced by the change of stray capacitance caused by the deformation of all components within the pressure vessel and the vessel itself, but this influence is negligible for the capacitor design discussed above.) The capacitance of an ideal cylindrical capacitor is given by $C_{\text{cyl}} = 2\pi\varepsilon l/\ln(d_o/d_i)$ with ε being the dielectric constant, l the electrode length, d_o the inner diameter of the outer electrode, and d_i the outer diameter of the inner electrode. Thus, only the relative change $\Delta l(p)/l(p = 0)$ of l is relevant, i.e. κ_{eff} is about one third of the volume compressibility κ_{vol} of the electrode material, which is the inverse of the bulk modulus.

The elastic property κ_{vol} has been determined for tungsten carbide with resonant ultrasound spectroscopy (RUS) [11, 12], which uses normal-mode resonance frequencies of free vibration as well as data on the shape and the mass of the sample. The experimental setup used and procedure have already been described in detail in [9, 13]. For each of the two capacitor materials, measurements near the TPW temperature were performed on 12 parallelepipeds made of tungsten carbide from the same sinter–powder mixture, from which the capacitor electrodes were manufactured. The dimensions of the three groups of test samples were approximately $17 \times 13 \times 10\,\text{mm}^3$, $13 \times 10 \times 9\,\text{mm}^3$, and $12.5 \times 11 \times 8\,\text{mm}^3$, respectively. The uncertainty of the result for each sample was determined individually using Monte-Carlo simulations, in which the input parameters were varied corresponding to their uncertainty

[2] Identification of commercial equipment and materials in this paper does not imply recommendation or endorsement by PTB, nor does it imply that the equipment and materials identified are necessarily the best available for the purpose.

Table 1. Uncertainty budgets for the determination of the composite effective compressibilities κ_{TC2} and κ_{TC3} of the capacitors TC2 and TC3. The numbers for TC1 from [1, 3] are given for comparison. The estimates for the relative uncertainties are given in %.

Component	TC1	TC2	TC3
Determination of the adiabatic compressibility of the electrode materials from RUS frequencies (RPR ↔ FEM)	0.056	0.024	0.017
Determination of the adiabatic compressibility of the electrodes from the density dependence (not for TC1)	0.087	0.006	0.096
Conversion between adiabatic and isothermal compressibility	0.041	0.041	0.038
Displacement correction	0.130	0.003	0.015
Compressibility of the insulation disks	0.012	0.002	0.002
Combined standard uncertainty	0.171	0.048	0.106

estimates. In both cases, the resulting data for the dependence of κ_{vol} on the density ρ were approximated by a linear fit function. This allowed the determination of individual κ_{vol} values for the electrodes by inserting the ρ values into the respective fit function. The ρ values were deduced from the measured masses (standard uncertainty 1 mg for masses up to 200 g) and dimensions (standard uncertainty of 1 μm for lengths of order 20 mm). The described procedure together with the improvement in dimensional measurement led to a reduction in uncertainty compared to [1] (see table 1) for TC2. For TC3 this was not the case because the uncertainty of the κ_{vol} determination still depends on the individual electrode and the individual density.

The determination of the adiabatic compressibility of the electrodes from RUS frequencies is an inverse problem, the uncertainty of which is primarily limited by the uncertainty of the dimensions of the sample. It starts with the forward problem, which means the calculation of resonance frequencies of free elastic vibrations of a sample with given geometry, known mass density and elastic coefficients. The calculated frequencies are then compared with the measured spectrum. In an iterative process, the input parameters have to be adjusted during each iteration step to minimize the error function, which is defined as the square sum of the differences between the calculated and measured frequencies. Except for some particularly simple cases, the calculation of resonance frequencies cannot be solved analytically, but it can be turned into an eigenvalue problem by the use of proper numerical methods. Based on the Rayleigh–Ritz method, Visscher *et al* [14] established for simple sample shapes (parallelepiped blocks, spheres and cylinders) a computational scheme for the free vibration of a sample with anisotropic properties. The inverse problem is a multi-dimensional nonlinear optimization problem. The Levenberg–Marquardt method may be considered as the standard nonlinear optimization method, which in conjunction with the Rayleigh–Ritz method has been implemented in the rectangular parallelepiped resonator (RPR) code designed by Migliori *et al* [12]. For estimating the uncertainty of the solution of the inverse problem, the results obtained with the RPR code and FEM were compared for all test samples.

It has to be considered that the compressibility κ_{vol} measured by RUS is the adiabatic one, whereas for the DCGT the isothermal κ_{vol} value is needed. For the conversion from the adiabatic to the isothermal κ_{vol} value, the well known formula of Grüneisen $\kappa_{isothermal} = \kappa_{adiabatic} + T\alpha_V^2/(\rho C_p)$ [15] was used. This requires values for ρ, the thermal-expansion coefficient α_V and the specific heat capacity C_p at constant pressure. For the two capacitor materials, the measured values are (with the relative standard uncertainty in parenthesis): $\alpha_{VTC2} = 1.314(45) \times 10^{-5}$ K^{-1}, $C_{pTC2} = 206.3(1.7)$ J kg^{-1} K^{-1}, $\alpha_{VTC3} = 1.299(45) \times 10^{-5}$ K^{-1}, $C_{pTC3} = 206.2(0.8)$ J kg^{-1} K^{-1}.

The displacement of the top surfaces of the inner and outer electrode under pressure is primarily caused by the difference in the compressibilities. The influence of this displacement has been calculated in two ways, namely by FEM and an analytic approximation. In the latter, it is considered that the capacitance between the longer electrode and the top surface of the shorter electrode decreases with increasing distance. This is simulated by a conical disk ranging from height zero near to the longer electrode up to the top surface of the longer electrode on the other side. The capacitance between the disk and the longer electrode can be calculated by integration [16]. To deduce the effective compressibility, the FEM result has been used. Its uncertainty has been estimated from the difference between the results obtained by both methods.

The uncertainty budgets for the effective compressibilities of the two new capacitors TC2 and TC3 are given in table 1 (the numbers for TC1 from [1, 3] are given for comparison). Although the capacitors are composite structures, the uncertainties are practically exclusively dominated by components connected with the electrodes. Taken from the literature, the properties of the sapphire discs (standard orientation: perpendicular to the *C*-axis) have negligible influence. The composite effective compressibilities of the two capacitors are: $\kappa_{TC2} = -9.352 \times 10^{-13}$ Pa^{-1} and $\kappa_{TC3} = -9.895 \times 10^{-13}$ Pa^{-1}.

2.4. Capacitance measurement

Considering the extreme demands concerning the measurement of capacitance changes, a high-resolution and high-precision autotransformer ratio capacitance bridge was built and tested. Its main component is a home-made high-precision 1:1 inductive voltage divider used in an autotransformer configuration. For balancing the bridge, adjustable in-phase and quadrature currents can be injected. A detailed uncertainty budget for measuring small capacitance changes is presented in [17]. Considering correlations between main terms in the mathematical model, it is shown that it is possible to measure capacitance changes of at most a few tenths of a percent with a relative standard uncertainty below one part per million, i.e. with a standard uncertainty relative to the capacitance value of order one part per billion. The performed consideration of

correlations requires that the measuring circuit be fully symmetric. For this reason, the reference capacitor is also located in the measuring system within the vacuum chamber.

To check the reliability of the uncertainty estimates experimentally, the results obtained with the newly developed bridge were compared with those obtained with the bridge applied previously for DCGT measurements in the low-temperature range; see [18] and the references cited therein. The preceding bridge, containing a variable home-made high-precision inductive voltage divider with nine decades, is described briefly in [19]. Within the upper ratio-error limits of the divider of 10 parts per billion (ppb), no discrepancies were found.

To achieve the required resolution it was necessary (i) to optimise the use of chokes as current equalisers based on a careful analysis of the capacitance measuring network as recommended in [20], (ii) to connect the low-level terminals of the measuring and reference capacitors inside the thermostat, i.e. only one cable goes to the null detector of the bridge at room temperature and, thus, the parasitic capacitance to ground is reduced, (iii) to use low-noise cables, (iv) to measure the unbalanced signal of the null detector with a bandwidth of order 0.01 Hz, and (v) to use switching between the capacitors inside the thermostat, reducing the influence of stray fields by additional shielding.

At all pressures, capacitance measurements were performed for the two opposite connections of the high-level terminals of the measuring and reference capacitors to the bridge. This yields information on the consistency of the data and the Type B uncertainty component of the inductive voltage divider caused by large-scale or 'integral' non-linearities. Furthermore, it increases the additional, statistical information on the short-range or 'differential' non-linearities of the inductive voltage divider decades used for balancing the bridge (Type A uncertainty component).

2.5. Pressure measurement

The goal of measuring pressures up to 7 MPa with a relative standard uncertainty of order 1 ppm is a challenge because it requires characterisation of pressure balances with unprecedented accuracy and even significant improvement of the national standard of PTB. For absolute pressure measurements in helium up to 7 MPa, a system of special pressure balances, as outlined in [21, 22], was designed, constructed and evaluated [2, 23–25]; see also the summary in [9]. The system includes two pressure-balance platforms, three piston-cylinder units (PCUs) with effective areas of 20 cm^2, and three 2 cm^2 PCUs. Traceability to the SI base units up to 7 MPa was realised in two steps. First, the zero pressure effective areas of the 20 cm^2 PCUs were determined from dimensional measurements. Second, the 2 cm^2 PCUs were calibrated against the 20 cm^2 PCUs by cross-float comparisons. The calibration of the mass pieces traceable to the national mass standards and the accurate determination of the local gravity acceleration did not represent special challenges. For the measuring gas, helium, the head correction due to the gas column was very small. Its overall relative magnitude for the present DCGT setup amounted only to 8 ppm.

2.6. Purity of the measuring gas

The determination of the Boltzmann constant at the TPW gives rise to extreme requirements regarding the purity of the measuring gas, helium. Impurities should not cause a relative change of the result by more than 1 ppm. To prevent contamination of the helium of nominal purity 99.999 99% during handling, the gas purifier (adsorber) Micro Torr SP70 from SAES Pure Gas, Inc., and the helium purifier (getter) HP2 from Valco Instruments, Co. Inc., were incorporated in the ultra-high-purity gas-handling system described in [1, 9]. (For the getter, the specified upper limit for water and the other relevant impurities besides noble gases is 10 ppb. For the adsorber, this value is 0.1 ppb.) After each measurement of an isotherm, which lasted usually one week, the measuring gas was analysed with the aid of a mass spectrometer (GAM 400, InProcess Instruments) to check for possible contamination especially due to outgassing from the different components inside the pressure vessel. The analysis was developed further by evaluating the spectra absolutely (without the self-correction of the spectrometer) and removing the background (noise and other parasitic signals) more efficiently by frequent switching between measuring gas from the capacitor and original gas from the supplied bottle. The detection limit for noble gas contamination is 10 ppb. The most problematic impurity is water because it has a polarizability 160 times larger than that of helium. Thus, the detection limit of 20 ppb would cause an uncertainty component of order 1 ppm applying a rectangular distribution. But additional analysis of helium gas remaining in the system for weeks led to an even lower uncertainty component. Therefore, considering the specification of the adsorber, 1 ppm is a reliable upper estimate for an overall uncertainty component including all relevant impurities.

3. Experimental results and data treatment

3.1. DCGT isotherms

A total of eight isotherms for both TC2 and TC3, respectively, were measured with helium from different bottles (nominal purity 99.999 99 %, supplier Linde AG). The mean temperature of all isotherms was $T_{mean} = 273.1576$ K (about 2 mK difference with the TPW) with a standard deviation of 1 mK over the whole measurement campaign lasting 12 months. (This statement demonstrates the very high temperature stability of the measuring system. It has no relevance for the traceability to the TPW temperature, because for the evaluation of each isotherm, the individual temperatures were used.) In the pressure range between 0.75 MPa and 6.7 MPa, 19 pairs of relative capacitance change and pressure were measured per isotherm. This led to a total of 152 triplets of temperature, pressure and relative capacitance change measured for each capacitor during the campaign. To check the possible influence of impurities caused by outgassing during the long time necessary for measuring one isotherm, additional single triplets were determined by evacuating and flushing the measuring capacitor between the measurements. No deviation from the isotherm data was detected. Also no differences

Table 2. Tabulated values A_{1TC2i} ($i = 1, 2, \ldots, 8$) obtained for capacitor TC2. The uncertainties $u(A_{1TC2i})$ are the standard uncertainties.

Isotherm	A_{1TC2i} (Pa)	$u(A_{1TC2i})$ (Pa)	Isotherm	A_{1TC2i} (Pa)	$u(A_{1TC2i})$ (Pa)
1	4396816119	17273	5	4396791934	23690
2	4396802001	20484	6	4396788943	25981
3	4396799093	19407	7	4396805176	22888
4	4396816776	17173	8	4396827816	18772

Table 3. Tabulated values A_{1TC3i} ($i = 1, 2, \ldots, 8$) obtained for capacitor TC3. The uncertainties $u(A_{1TC3i})$ are the standard uncertainties.

Isotherm	A_{1TC3i} (Pa)	$u(A_{1TC3i})$ (Pa)	Isotherm	A_{1TC3i} (Pa)	$u(A_{1TC3i})$ (Pa)
1	4397167639	25392	5	4397167267	19930
2	4397159059	24888	6	4397149581	23649
3	4397174768	20387	7	4397171251	23426
4	4397191966	27727	8	4397185550	22424

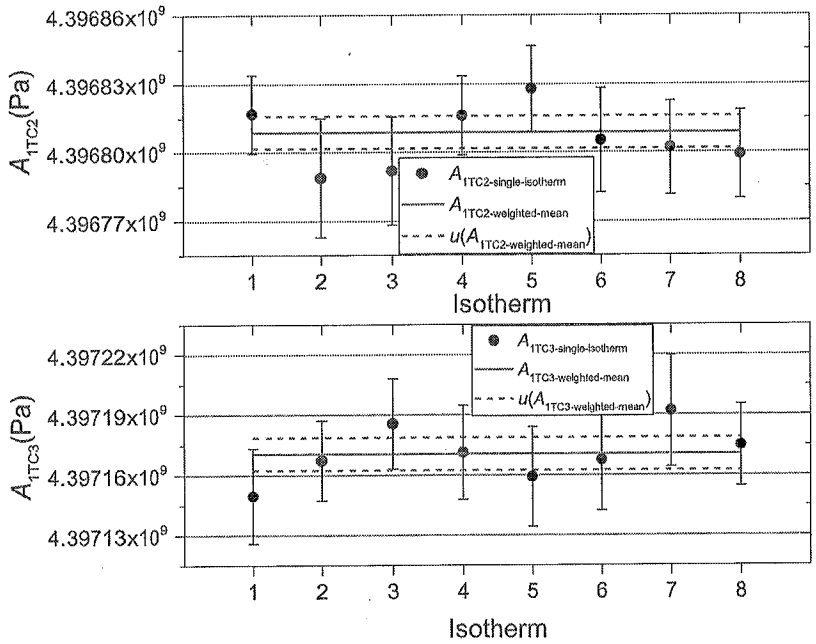

Figure 2. Isotherm fit results for the capacitors TC2 (upper plot) and TC3 (lower plot). The black points show the values of the coefficient A_1 resulting from a constrained third-order fit to the isotherm data, and the error bars are the standard uncertainty estimates deduced using the maximum-likelihood estimation [26]. In both plots, the red line shows the weighted-mean A_1 value, and the dashed lines show its standard uncertainty.

between isotherms measured with ascending or descending pressure changes were detected. This is a clear indicator that in the final design shown in figure 1, there is no evidence for hysteresis effects. These tests are also a proof of remaining gas purity (see section 2.6).

3.2. Evaluation of the DCGT isotherm data

The eight isotherms for each capacitor were first fitted individually by polynomials of fourth and fifth order according to the working equation derived in [3]. The uncertainty of the fitting parameters was deduced using maximum-likelihood estimation [26]. In the next step, the mean fourth fit coefficient a_4 from both capacitors was calculated via a weighted mean of all 32 a_4 values obtained from fourth- and fifth-order fits. (In the nomenclature of [3], a_4 is equal to the product $A_1 A_4$.) The weighted mean $a_{4\text{-weighted-mean}} = 2.52(27) \times 10^{13}$ Pa is in good agreement with the value $a_{4\text{-theory}} = 2.61 \times 10^{13}$ Pa derived from the latest *ab initio* calculations for the fourth virial coefficient of helium [27] by applying the DCGT working equation given in [3]. In a further step, $a_{4\text{-weighted-mean}}$ was used as a constraint for correcting the data. The final third-order fits were performed using the corrected isotherm data. This procedure guarantees that the influence of the fourth virial coefficient on A_1 is completely considered by the third-order fit. The uncertainty component arising from this procedure is correlated for the two capacitors TC2 and TC3. Since $a_{4\text{-weighted-mean}}$ was obtained by statistical methods, this is taken into account by a partial correlation of the Type A uncertainty estimates (see table 5 in section 4). The extracted values of coefficient A_1 of the linear term for the different isotherms corrected to the same temperature are listed in tables 2 and 3 for capacitors TC2 and TC3, respectively, and plotted in figure 2. It is obvious that, in both cases, the eight values agree well within their standard uncertainties. Therefore, it is possible to calculate the weighted mean of the eight

Table 4. Uncertainty budgets for the determination of the Boltzmann constant by DCGT at the TPW using capacitors TC2 and TC3. The estimates give the relative uncertainty components in ppm. The numbers for TC1 from [1, 3] are given for comparison.

Component	TC1	TC2	TC3
Type A estimate	2.62	1.60	1.86
Type B estimates			
Susceptibility measurement (capacitance change)	1.00	0.40	0.40
Determination of the effective compressibility κ_{eff}	2.35	0.65	1.53
Temperature (traceability to the TPW)	0.30	0.30	0.30
Pressure measurement (7 MPa)	1.00	1.00	1.00
Head correction (pressure of gas column)	0.20	0.20	0.20
Impurities (measuring gas)	1.00	1.00	1.00
Surface layers (impurities)	0.50	0.50	0.50
Polarizability from *ab initio* calculation (theory)	0.20	0.10	0.10
Combined standard uncertainty	3.97	2.36	2.89

Table 5. Qualitative overview of the correlations between the corrections $\delta k_{\text{TC}ki}$ ($k = 1, 2, 3$, $i = 1, 2, \ldots, 9$), which are connected with the different components of the individual uncertainty budgets, for the three capacitors TC1, TC2 and TC3.

i	Component	Correlation
1	Type A estimate	Partial
2	Susceptibility measurement (capacitance change)	Complete
3	Determination of the effective compressibility κ_{eff}	Partial
4	Temperature (traceability to the TPW)	Complete
5	Pressure measurement (7 MPa)	Complete
6	Head correction (pressure of gas column)	Complete
7	Impurities (measuring gas)	No (independent)
8	Surface layers (impurities)	No (independent)
9	Polarizability from *ab initio* calculation (theory)	Complete

individual A_1 values for each capacitor. The two weighted means are $A_{1\text{TC2-weighted-mean}} = 4.396\,808\,8(71) \times 10^9$ Pa and $A_{1\text{TC3-weighted-mean}} = 4.397\,1706(82) \times 10^9$ Pa. Together with the isotherm temperature and the κ_{eff} value deduced in section 2.3, this leads to a ratio A_ε/R of $6.221\,1484 \times 10^{-8}\text{m}^3\ \text{K}\ \text{J}^{-1}$ for TC2 and $6.221\,1316 \times 10^{-8}\ \text{m}^3\ \text{K}\ \text{J}^{-1}$ for TC3. Finally, applying the relation $k = (\alpha_0/\varepsilon_0)/(3\ A_\varepsilon/\ R)$, the two values $k_{\text{TC2}} = 1.380\,6464 \times 10^{-23}\ \text{J}\ \text{K}^{-1}$ and $k_{\text{TC3}} = 1.380\,6501 \times 10^{-23}\ \text{J}\ \text{K}^{-1}$ were obtained for the Boltzmann constant (see also table 8). The uncertainty budgets for k_{TC2} and k_{TC3} are given in table 4. In the present work as well as in [1] single isotherm data were fitted, because this corresponds to the original form of the measurement. Nevertheless, global fits to the data for both capacitors proved the consistency of the results for k and the given uncertainties.

3.3. Uncertainty budgets

The complete uncertainty budgets for the determination of the Boltzmann constant by DCGT at the TPW applying capacitors TC2 and TC3, respectively, are given in table 4 (the numbers for TC1 from [1, 3] are given for comparison). They have been established in accordance with the *Guide to the Expression of Uncertainty in Measurement* [28].

In both cases, the Type A uncertainty component is estimated by the uncertainty of the weighted mean of the $A_{1\text{TC}ki}$ values ($i = 1, 2, \ldots, 8$). It includes the scatter of the averaged unbalanced output signal of the capacitance bridge, the pressure repeatability, and the instability of temperature and capacitance. In the Type B estimate for the susceptibility measurement via capacitance changes, only the large scale or 'integral' non-linearities of the capacitance bridge are considered in accordance with [17], since the short-range or 'differential' non-linearities are contained in the Type A estimate. (In the budgets presented in [1, 3], a double counting of the 'differential' non-linearities in the Type A and Type B estimates was accepted in view of the dominance of other uncertainty components.) The instability of the capacitance of the measuring capacitor (drift during the measurement of an isotherm lasting several days, influence of pressure cycling) contributes also to this Type B estimate. Uncertainty budgets for the determination of the effective compressibilities κ_{TC2} and κ_{TC3} of capacitors TC2 and TC3, respectively, are established in section 2.3. The component estimated for the temperature measurement includes static and dynamic errors within the measuring system; see section 2.1. The estimates connected with the pressure measurement and the head correction are discussed in section 2.5. Impurities cause errors since their polarizability differs from that of helium; see the discussion in section 2.6. Surface layers on the electrodes of the measuring capacitor play a minor role because they are present both for the measurement with the helium gas and with vacuum. Calculations of further higher-order QED corrections for the static dipole polarizability [4] lead to a decreased uncertainty of 0.1 ppm compared to [29] used in [1]. (Possible variations of the isotopic composition of the measuring gas helium do not cause any problems because the natural abundance of the light isotope ^{3}He is only 1.3 ppm and the relative deviation of the polarizabilities of the two isotopes amounts only to about 0.01%.)

4. Combination of different k values taking correlations into account

The final result for the Boltzmann constant was obtained by applying the formulas given in the appendix for determining the weighted mean of the $m = 3$ values k_{TC1}, k_{TC2} and k_{TC3}

Table 6. Analysis of the significant correlations between sub-corrections in determining the effective compressibility of the three capacitors TC1, TC2 and TC3. For each capacitor pair, it is stated whether a sub-correction is correlated ('yes') or not ('no').

Sub-correction	TC1 ↔ TC2	TC1 ↔ TC3	TC2 ↔ TC3
Determination of the adiabatic compressibility of the electrodes from RUS frequencies (RPR ↔ FEM)	Yes	Yes	Yes
Conversion between adiabatic and isothermal compressibility	Yes	No	No
Displacement correction	No	No	Yes

Table 7. Relative covariance matrix V for the three values k_{TC1}, k_{TC2} and k_{TC3} measured with the capacitors TC1, TC2 and TC3. The figures are given in ppm^2.

	TC1	TC2	TC3
TC1	15.8	2.1	1.7
TC2	2.1	5.6	1.5
TC3	1.7	1.5	8.3

measured with the capacitors TC1, TC2 and TC3, respectively, taking correlations into account. The value k_{TC1} and the budget for its uncertainty have been taken from [3]. Table 5 gives a qualitative overview of the correlations between the $n = 9$ corrections, which are connected with the different components of the individual uncertainty budget.

The partial correlation of the Type A corrections δk_{TC21} and δk_{TC31} is caused by the constraint considering the influence of the fourth-order term of the virial expansion in fitting the isotherm data, see section 3.2. This constraint was obtained for the two capacitors TC2 and TC3 together by applying statistical methods (fits to repeated isotherms with several data for different pressures). Most complicated is the analysis of the correlations for the third correction $\delta k_{TCk3} = \delta k_{TCk,\kappa_{eff}}$, for which detailed formulas are given in the appendix. This correction is the sum of different sub-corrections depending on several quantities x_j. For the three capacitor pairs, table 6 gives an individual analysis of the significant correlations.

The results of the correlation analysis are presented in tables 7 and 8. (The number of digits of the figures in the two tables has been chosen so that the final result can be closely reproduced.) Table 7 is the relative covariance matrix V defined in equation (A.9) of the appendix. The correlation coefficients are: $r(k_{TC1}, k_{TC2}) \approx 0.23$, $r(k_{TC1}, k_{TC3}) \approx 0.15$ and $r(k_{TC2}, k_{TC3}) \approx 0.22$. Table 8 contains, besides the three values k_{TC1}, k_{TC2} and k_{TC3} and their relative standard uncertainties, the weights without (w_{wout}) and with (w_{with}) consideration of correlations. The weighted mean with correlations amounts to $k_{WM} = 1.3806482 \times 10^{-23}$ J K^{-1} with a relative standard uncertainty of $u(k_{WM}) = 1.9$ ppm. In figure 3, k_{TC1}, k_{TC2} and k_{TC3} are compared with k_{WM}. In all three cases, the deviation from the weighted mean is well within the combined uncertainties.

Table 8. Results necessary for calculating the weighted mean k_{WM} of the values k_{TC1}, k_{TC2} and k_{TC3} taking correlations into account. The estimates u_r are the relative standard uncertainties of the three values. The weights w_{with} with consideration of correlations are deduced from the weight matrix W, which is the inverse of the covariance matrix V given in table 7; see the appendix. The weights w_{wout} were obtained directly from the estimates u_r, i.e. without considering correlations. The resulting weighted-mean values k_{wout} and $k_{with} = k_{WM}$ are given together with their relative standard uncertainties for comparison.

	k_{TCi} (10^{-23} J K^{-1})	u_r (ppm)	w_{wout}	w_{with}
k_{TC1}	1.3806509	3.97	0.175	0.131
k_{TC2}	1.3806464	2.36	0.493	0.542
k_{TC3}	1.3806501	2.89	0.333	0.327
k_{wout}	1.3806484	1.66		
$k_{with} = k_{WM}$	1.3806482	1.94		

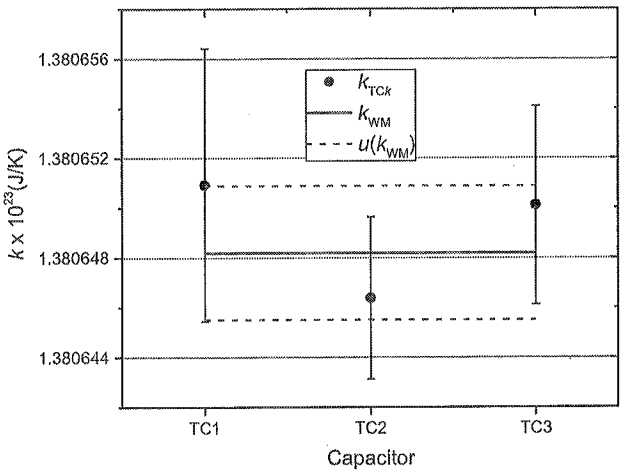

Figure 3. Comparison of the three values k_{TC1}, k_{TC2} and k_{TC3} of the Boltzmann constant measured with the capacitors TC1, TC2 and TC3 (dots), respectively, with the weighted mean k_{WM} deduced taking correlations into account (solid line). The dashed lines show the standard uncertainty of k_{WM}.

5. Conclusions

Based on a huge amount of data, two new values of the Boltzmann constant k have been obtained by DCGT by applying two different highly stable tungsten-carbide capacitors. The combination of these with the value published in 2013 taking correlations fully into account yielded a final result of $k = 1.3806482 \times 10^{-23}$ J K^{-1} with a relative standard uncertainty of 1.9 ppm. This value is about 0.2 ppm smaller than the CODATA 2014 result [5], which has a relative standard uncertainty of 0.57 ppm. In addition, the uncertainty and the value presented here are comparable to those of the outstanding experiment with a spherical acoustic resonator that defined the value of k for more than two decades [30].

The reduction of the uncertainty of the final result by a factor two compared with the result published in 2013 has been mainly achieved by three advances: (i) improvement of the mounting of the capacitor electrodes and attenuation of the influence of stray fields by additional shielding, which led to a better stability and thus a smaller Type A uncertainty component for the two

new capacitors; (ii) determination of the individual adiabatic compressibility of the electrodes from the carefully analysed density dependence, which resulted in an essentially smaller uncertainty of the effective compressibility, especially for one of these capacitors; (iii) inclusion of many more experimental results by combining the data obtained for the three capacitors.

The final determination of the Boltzmann constant with DCGT meets the last remaining requirement of the Consultative Committee for Thermometry for a new definition of the kelvin, namely to have independent determinations of k with a relative standard uncertainty below 3 ppm by applying at least two fundamentally different methods. Consequently, the result of the decennial project paves the way for the new definition of the base unit kelvin by fixing the k value.

Acknowledgments

We thank Sebastian Bronkalla for his technical support in building the setup during the whole project.

Appendix. Weighted mean of correlated DCGT data and its uncertainty

The evaluation of correlated data is universally treated in the appendices of the paper 'CODATA recommended values of the fundamental physical constants: 1998' by Mohr and Taylor 2000 [31]. In the present paper, this basic theory is applied to the example of the determination of the Boltzmann constant by DCGT.

The linearised mathematical model of the measurement result for the Boltzmann constant obtained with capacitor assembly No. TCk is

$$k_{\mathrm{TC}k} = k_{\mathrm{TC}k0} + \sum_{i=1}^{n} \delta k_{\mathrm{TC}ki}, \quad k = 1, 2, \ldots, m \qquad \text{(A.1)}$$

with the ideal gas term

$$k_{\mathrm{TC}k0} = \frac{\alpha_0}{3\varepsilon_0} \frac{1}{T_{\mathrm{TPW}}\left(\frac{1}{A_{1\mathrm{TC}k}} - \frac{\kappa_{\mathrm{TC}k}}{3}\right)} \qquad \text{(A.2)}$$

(α_0 is the static electric dipole polarizability of the gas particles, ε_0 is the fixed electrical constant, T_{TPW} is the defined fixed-point temperature of the TPW ($T_{\mathrm{TPW}} = 273.16\,\mathrm{K}$), $A_{1\mathrm{TC}k}$ is the coefficient of the linear term of the virial expansion fitted to the isotherm data, $\kappa_{\mathrm{TC}k}$ is the effective compressibility of the capacitor assembly TCk) and the sum of n correction terms. The correction terms $\delta k_{\mathrm{TC}ki}$ are connected with the different components of the individual uncertainty budget. It is assumed that the corrections of one measurement result are independent of the others. This means for their covariances:

$$\mathrm{cov}(\delta k_{\mathrm{TC}ki}, \delta k_{\mathrm{TC}li}) \neq 0 \quad \text{and} \quad \mathrm{cov}(\delta k_{\mathrm{TC}ki}, \delta k_{\mathrm{TC}lj}) = 0 \text{ for } i \neq j. \qquad \text{(A.3)}$$

The covariances of the corrections $\mathrm{cov}(\delta k_{\mathrm{TC}ki}, \delta k_{\mathrm{TC}li})$ have to be determined via error propagation with sensitivity coefficients or Monte Carlo simulation by applying the formulas used for their estimation. Then, the covariance of two values of the Boltzmann constant is given by a sum of covariances

$$\mathrm{cov}(k_{\mathrm{TC}k}, k_{\mathrm{TC}l}) = \sum_{i=1}^{n} \mathrm{cov}(\delta k_{\mathrm{TC}ki}, \delta k_{\mathrm{TC}li}) \qquad \text{(A.4)}$$

with $\mathrm{cov}(k_{\mathrm{TC}k}, k_{\mathrm{TC}k}) = u^2(k_{\mathrm{TC}k})$ (u is the standard uncertainty).

It is assumed that the ith correction term depends on the q quantities $x_1, x_2, \ldots, x_q$:

$$\delta k_{\mathrm{TC}ki} = f_{\mathrm{TC}ki}(x_1, x_2, \ldots, x_q). \qquad \text{(A.5)}$$

The dependences may differ for the different experimental results. Linearisation of the mathematical model for considering the uncertainties of these quantities yields for the covariance of the ith correction terms of the kth and lth experimental result:

$$\mathrm{cov}(\delta k_{\mathrm{TC}ki}, \delta k_{\mathrm{TC}li}) = \sum_{j=1}^{q} \left(\frac{\partial f_{\mathrm{TC}ki}}{\partial x_j}\right)\left(\frac{\partial f_{\mathrm{TC}li}}{\partial x_j}\right) u^2(x_j). \qquad \text{(A.6)}$$

For instance, the formula for the correction term caused by the uncertainty of the effective compressibility κ_{eff} is given by

$$\mathrm{cov}\left(\frac{\delta k_{\mathrm{TC}k,\kappa_{\mathrm{eff}}}}{k_{\mathrm{TC}k,\kappa_{\mathrm{eff}}}}, \frac{\delta k_{\mathrm{TC}l,\kappa_{\mathrm{eff}}}}{k_{\mathrm{TC}l,\kappa_{\mathrm{eff}}}}\right) = \frac{1}{9\kappa_{\mathrm{TC}k}\kappa_{\mathrm{TC}l}((A_{1\mathrm{TC}k}\kappa_{\mathrm{TC}k})^{-1} - 1/3)((A_{1\mathrm{TC}l}\kappa_{\mathrm{TC}l})^{-1} - 1/3)} \sum_{j=1}^{q} \left(\frac{\partial \kappa_{\mathrm{TC}k}}{\partial x_j}\right)\left(\frac{\partial \kappa_{\mathrm{TC}l}}{\partial x_j}\right) u^2(x_j) \approx$$

$$\frac{A_{1\mathrm{TC}k}A_{1\mathrm{TC}l}}{9} \sum_{j=1}^{q} \left(\frac{\partial \kappa_{\mathrm{TC}k}}{\partial x_j}\right)\left(\frac{\partial \kappa_{\mathrm{TC}l}}{\partial x_j}\right) u^2(x_j). \qquad \text{(A.7)}$$

This can be transformed into the following equation:

$$\mathrm{cov}\left(\frac{\delta k_{\mathrm{TC}k,\kappa_{\mathrm{eff}}}}{k_{\mathrm{TC}k,\kappa_{\mathrm{eff}}}}, \frac{\delta k_{\mathrm{TC}l,\kappa_{\mathrm{eff}}}}{k_{\mathrm{TC}l,\kappa_{\mathrm{eff}}}}\right) \approx \frac{A_{1\mathrm{TC}k}A_{1\mathrm{TC}l}\kappa_{\mathrm{TC}k}\kappa_{\mathrm{TC}l}}{9} \sum_{j=1}^{q} \frac{u_{x_j}(\kappa_{\mathrm{TC}k})}{\kappa_{\mathrm{TC}k}} \frac{u_{x_j}(\kappa_{\mathrm{TC}l})}{\kappa_{\mathrm{TC}l}}. \qquad \text{(A.8)}$$

The quadratic $m \times m$ covariance matrix $\boldsymbol{V}$ and its inverse matrix, the weight matrix $\boldsymbol{W}$, are defined by

$$\boldsymbol{V} = (\mathrm{cov}(k_{\mathrm{TC}k}, k_{\mathrm{TC}l}))_{m,m} = (v_{kl})_{m,m} \text{ and } \boldsymbol{W} = (w_{kl})_{m,m} = \boldsymbol{V}^{-1}. \qquad \text{(A.9)}$$

The correlation coefficients are given by $r(k_{\mathrm{TC}k}, k_{\mathrm{TC}l}) = \mathrm{cov}(k_{\mathrm{TC}k}, k_{\mathrm{TC}l})/(u(k_{\mathrm{TC}k})u(k_{\mathrm{TC}l}))$. With these definitions, the expression for the weighted mean $\widehat{k}$ of the m results for the Boltzmann constant is the following double sum (in

accordance with equation (E26) in the paper by Mohr and Taylor [31]):

$$\widehat{k} = \frac{1}{G} \sum_{l=1}^{m} k_{\mathrm{TCI}} \sum_{k=1}^{m} w_{kl}. \tag{A.10}$$

with $G = \sum_{l=1}^{m} \sum_{k=1}^{m} w_{kl}$ and $\frac{1}{G} \sum_{k=1}^{m} w_{kl}$ being the weights. The double sum G yields the standard uncertainty of $\widehat{k}$ (see equation (E27) in the paper by Mohr and Taylor [31]):

$$u(\widehat{k}) = \sqrt{\frac{1}{G}}. \tag{A.11}$$

References

[1] Gaiser C *et al* 2013 *Metrologia* **50** L7–11
[2] Zandt T *et al* 2015 *Metrologia* **52** S305–13
[3] Gaiser C *et al* 2015 *Metrologia* **50** S217–26
[4] Piszczatowski K *et al* 2015 *Phys. Rev. Lett.* **114** 173004
[5] Mohr P J *et al* 2016 *Rev. Mod. Phys.* **88** 035009
[6] Zandt T *et al* 2010 *Int. J. Thermophys.* **31** 1371–85
[7] Zandt T *et al* 2011 *Int. J. Thermophys.* **32** 1355–65
[8] Merlone A *et al* 2010 *Int. J. Thermophys.* **31** 1386–95
[9] Fellmuth B *et al* 2011 *Metrologia* **48** 382–90
[10] Thoma P 1966 *Arch. Elektrotech.* **50** 395–400
[11] Maynard J D 1992 *J. Acoust. Soc. Am.* **91** 1754–62
[12] Migliori A *et al* 1993 *Physica* B **183** 1–24
[13] Zandt T *et al* 2013 *AIP Conf. Proc.* **1552** 130–5
[14] Visscher W M *et al* 1991 *J. Acoust. Soc. Am.* **90** 2154–62
[15] Grüneisen E 1908 *Ann. Phys., Lpz.* **26** 394–402
[16] Röder G 2010 *Kapazitive Messung von Innendurchmessern* https://kluedo.ub.uni-kl.de/frontdoor/index/index/docId/2264
[17] Fellmuth B *et al* 2011 *IEEE Trans. Instrum. Meas.* **60** 2522–6
[18] Gaiser C *et al* 2017 *Metrologia* **54** 141
[19] Luther H *et al* 1996 *Metrologia* **33** 341–52
[20] Awan S *et al* 2011 *Coaxial Electrical Circuits for Interference-Free Measurements* (London: The Institution of Engineering and Technology)
[21] Sabuga W 2011 *PTB-Mitt.* **121** 247–55
[22] Sabuga W *et al* 2011 *PTB-Mitt.* **121** 256–9
[23] Sabuga W *et al* 2011 *PTB-Mitt.* **121** 260–2
[24] Sabuga W *et al* 2012 *Measurement* **45** 2464–8
[25] Priruenrom T 2011 *Development of Pressure Balances for Absolute Pressure Measurement in Gases up to 7 MPa* (Clausthal-Zellerfeld: Papierflieger Verlag)
[26] Fahrmeir L *et al* 2009 *Regression Modelle, Methoden und Anwendungen* 2nd edn (Berlin: Springer) pp 90–110
[27] Shaul K R S *et al* 2012 *J. Chem. Phys.* **137** 184101
[28] JCGM 100:2008 *Evaluation of Measurement Data—Guide to the Expression of Uncertainty in Measurement*
[29] Łach G *et al* 2004 *Phys. Rev. Lett.* **92** 233001–4
[30] Moldover M R *et al Phys. Rev. Lett.* **60** 249–52
[31] Mohr P J and Taylor B N 2000 *Rev. Mod. Phys.* **72** 351–495